

Thermal and Electrical Transport in Hybrid Woven Composites Reinforced with Aligned Carbon Nanotubes

Namiko Yamamoto¹, Roberto Guzman deVilloria², Hulya G. Cebeci¹, and Brian L. Wardle³
Massachusetts Institute of Technology, Cambridge MA 02139

Carbon nanotubes (CNTs) are a potential new component to be incorporated into existing aerospace structural composites for multifunctional (mechanical, electrical, thermal, etc.) property enhancement. Although CNT properties are extraordinary when measured individually, they tend to degrade by a large factor when integrated in system (often in polymer matrices). Mechanisms and effectiveness of nano-scale CNT implementation into macro-scale structural composites are not well understood. Non-mechanical aspects of these composites are the focus of this work. As a CNT hybridized fiber polymer composite, fuzzy fiber reinforced plastic (FFRP) is developed using a scalable fabrication method that achieves uniform CNT distributions for thermal and electrical conductive networks without requiring intensive mixing which can damage CNTs. At small CNT volume fractions ($\sim 0.5\text{-}8\% V_f$), characterization shows significant enhancement in electrical conduction ($\times 10^6\text{-}10^8$) but limited enhancement in thermal conduction ($\times 1.9$). In addition, aligned-CNT polymer nanocomposites (A-CNT-PNCs) are being characterized as a representative volume element (RVE) of the FFRP. Experimentally obtained data on consistent A-CNT-PNC samples sets provide engineering knowledge and to achieve effective utilization of CNTs' multifunctional properties. Theoretical studies, both analytical and numerical, have been recently developed, suggesting interface effects may be a key to explaining the above limitations, including electron tunneling/hopping or phonon scattering at CNT-CNT and CNT-polymer interfaces. Multiple test techniques and property extraction methods for A-CNT-PNCs are developed and/or employed for cross-comparison. Applications of nano-engineered composites enhanced with CNTs can include lightning protection layers, electromagnetic interference shields, thermal management layers, and thermoelectrical sensor layers for airplane structures.

I. Introduction

Carbon nanotubes (CNTs) can be potentially organized into existing aerospace structural composites to enhance multiple (structural, electrical, thermal, and etc.) properties. Existing aerospace structural composites are tailored with plies of aligned advanced fibers (usually carbon) in a polymer (usually epoxy), achieving high mass-specific strengths and moduli. While usage of such composites reduces the structural mass by up to $\sim 50\%$ compared with usage of light metal (e.g., aluminum) to achieve the equivalent mechanical properties [1], additional parts and thus masses are still added to the system to compensate for composites' non-mechanical properties. For example, carbon fiber reinforced plastics have relatively low electrical conductivity ($\sim 10\text{-}10^2$ S/m in the in-plane and ~ 1 S/m for through-thickness direction [2, 3], thus $\times 10^6\text{-}10^4$ of copper [4]). Enhanced electrical conduction is required for airplane structures to discharge lightning currents away from critical areas or to shield against electromagnetic (EM) interference from high power transmitters [5, 6]. Thus, airplane structures made of composites are commonly overwrapped with additional metal layers or metal-coated layers (copper fabric, etc.), which adds ~ 0.4 kg/m² weight [7]. In addition, thermal conductivity of fiber-matrix composites is low (~ 1 W/mK in the in-plane and ~ 0.1 W/mK in the through-thickness direction [2, 8-12], $\times 10^3\text{-}10^2$ of metals [4]). In the areas of high heat buildup (such as

¹ Graduate Student, Department of Aeronautics and Astronautics, 77 Massachusetts Ave, Cambridge MA 02139, and AIAA Member.

² Postdoctoral Associate, Department of Aeronautics and Astronautics, 77 Massachusetts Ave, Cambridge MA 02139, and AIAA Member.

³ Associate Professor, Department of Aeronautics and Astronautics, 77 Massachusetts Ave, Cambridge MA 02139, and AIAA Senior Member.

electric boards, engines, and aerodynamically heated sections), heat dissipation needs to be enhanced by the addition of management layers or thermal interface materials (TIMs).

CNTs, hybridized into existing advanced composites, offer a new solution to these systems. Unlike external metal layers that add weight, CNTs can enhance multi-functional properties of composites with minimum weight or process addition [13-15]. Due to their strong carbon-carbon bonding and their flawless atomic structure, CNTs have multiple exceptional properties; high mechanical stiffness and strength, thermal and electrical conductivities comparable with or higher than metals [16-18]. In addition, CNT density ($\sim 1.4 \text{ mg/mm}^3$ for single-walled carbon nanotubes [19-21]) is lower than metals, suggesting a good fit with mass-specific properties required in aerospace applications. The high aspect ratio of CNTs is advantageous to form a physical network throughout the structure that works as electrical and thermal conductive pathways [14, 22] and mechanical (especially inter-ply) connections [13-15, 23-25]. This work is motivated by application of the new nano-engineered, multi-scale, and multifunctional CNT-composites with various electro-thermal properties, such as deicing/anti-icing heaters or as system health monitors based on crack-induced resistance changes for airplane surface [26].

While many applications are anticipated, little has been thoroughly investigated for nano-scale CNT ($\sim 10^{-9} \text{ m}$ diameter) implementation in macro-scale composites ($\sim 10^{-4}$ – 10^{-2} m ply thickness and ~ 1 - 10 m structural dimension). In Fig. 1, thermal and electrical conductivities of CNTs and CNTs embedded in polymer at room temperature from the past literatures are summarized and are compared with other materials. The conductivities show large variability, and enhancement by CNTs in polymers is lower than expected, particularly in the case of thermal conduction. Large variation in measured values can be attributed to many factors, including CNTs themselves (quality/defects, diameter, chirality, length in comparison with electron mean free path, inter-shell transport, etc.), CNT morphologies (dispersion, volume fraction, and inter-tube resistance), and experimental uncertainties in sample preparation, test setup, and data analysis (Schottky barrier at electrodes, thermal resistances at interfaces, and elimination of these parasitic values in data analysis). Up to today, numerous explanations for such phenomenon are proposed, but none have been validated because consistent and comparable experimental data are currently missing. For successful designs of CNT implemented composites with highly improved conductivities, preparation of consistent, well-characterized sample sets and their proper measurement are necessary to understand the effects by CNT morphology or by polymer, including inter-CNT and CNT-polymer contact thermal boundary resistance (TBRs).

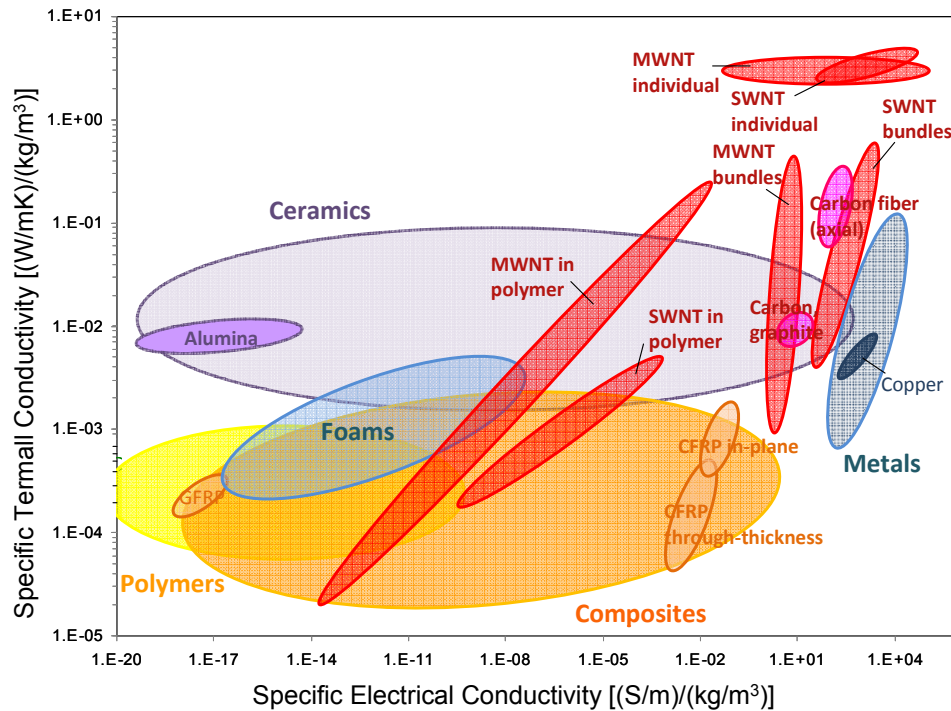


Figure 1. Electrical and thermal conductivities at room temperature normalized by density, following the format of Ashby charts [2]. CNT data points are the maximum and minimum measured values in literature.

In order to fill in the identified significant gaps in the extant work reviewed above, combined experimental and theoretical investigations on thermal and electrical properties of two types of samples are considered: aligned carbon nanotubes infiltrated with polymer (aligned CNT polymer nanocomposites, A-CNT-PNC [27][28]) and CNT hybridized fiber-polymer composites (fuzzy fiber reinforced plastics, FFRPs [14]), as shown in Fig. 2. A-CNT-PNCs are representative volume element (RVE), building block, of FFRPs, and are studied to better understand transport behaviors in the complex FFRP 3D morphologies [29]. In addition, not just as an RVE of FFRPs, A-CNT-PNCs by themselves can be used for thermal interface materials for electrical packaging applications [30]. These two types of samples, FFRPs and A-CNT-PNCs, are carefully fabricated to attain CNT alignments, are characterized using suitable methods to eliminate errors and uncertainties, sometimes encountered especially in measurement with small samples. These well-characterized samples with variable properties (volume fraction, length, etc.) provide comparable data sets with each other and with theoretical work, to quantitatively obtain critical properties to evaluate effectiveness of CNT addition. Key bottleneck factors for transport, such as boundary resistances between CNTs or between CNTs and polymer, can be extracted based on these data, which are critical to tailor and optimize nano-engineered composites suitable for various applications.

It is important to control CNT implementation into polymer matrices, as the CNT addition processing step (CNT mixture [31] and matrix cure [32]) can have a large influence on resulting composite properties. However, controlled CNT implementation is not simple. Most commonly, CNTs are simply mixed into polymer matrices, but good dispersion is not obtained due to van der Waals forces between CNTs. Intensive mixing (such as calendaring [33]) breaks and damages CNTs. Full quantitative characterization of CNT morphology in such nanocomposites (alignment, volume fraction, dispersion, etc.) is currently impossible, even with characterizations such as electron microscopy (scanning and transmission) and atomic force microscopy for images, Raman microscopy for crystallinity, and X-ray scattering for alignment [20]. Furthermore, measurements of CNT nanocomposites (often in thin film form) still requires much improvement to eliminate contact resistances and to ensure proper dimensional normalization [34]. Meanwhile, CNT addition into structural advanced fiber (ceramic [14], glass [22], and carbon [35, 36]) composites has been only recently investigated. Previously, such composites have been fabricated by either mixing CNTs into a polymer [22], by CNT deposition on fibers by electrophoresis [35], or by direct CNT growth on fiber cloth surfaces. In both CNT-PNC and CNT-advanced fiber composite cases, most work showed minimal property enhancement, and several even resulted in property degradation due to defects from improper CNT dispersion [36] or fiber damage from CNT growth on their surfaces [37-39]. Besides, to aim for industrial-level production, manufacturing processes should be carefully designed to achieve scalability, low cost, integration with existing processing, and minimal environmental contamination.

It is important to control CNT implementation into polymer matrices, as the CNT addition processing step (CNT mixture [31] and matrix cure [32]) can have a large influence on resulting composite properties. However, controlled CNT implementation is not simple. Most commonly, CNTs are simply mixed into polymer matrices, but good dispersion is not obtained due to van der Waals forces between CNTs. Intensive mixing (such as calendaring [33]) breaks and damages CNTs. Full quantitative characterization of CNT morphology in such nanocomposites (alignment, volume fraction, dispersion, etc.) is currently impossible, even with characterizations such as electron microscopy (scanning and transmission) and atomic force microscopy for images, Raman microscopy for crystallinity, and X-ray scattering for alignment [20]. Furthermore, measurements of CNT nanocomposites (often in thin film form) still requires much improvement to eliminate contact resistances and to ensure proper dimensional normalization [34]. Meanwhile, CNT addition into structural advanced fiber (ceramic [14], glass [22], and carbon [35, 36]) composites has been only recently investigated. Previously, such composites have been fabricated by either mixing CNTs into a polymer [22], by CNT deposition on fibers by electrophoresis [35], or by direct CNT growth on fiber cloth surfaces. In both CNT-PNC and CNT-advanced fiber composite cases, most work showed minimal property enhancement, and several even resulted in property degradation due to defects from improper CNT dispersion [36] or fiber damage from CNT growth on their surfaces [37-39]. Besides, to aim for industrial-level production, manufacturing processes should be carefully designed to achieve scalability, low cost, integration with existing processing, and minimal environmental contamination.

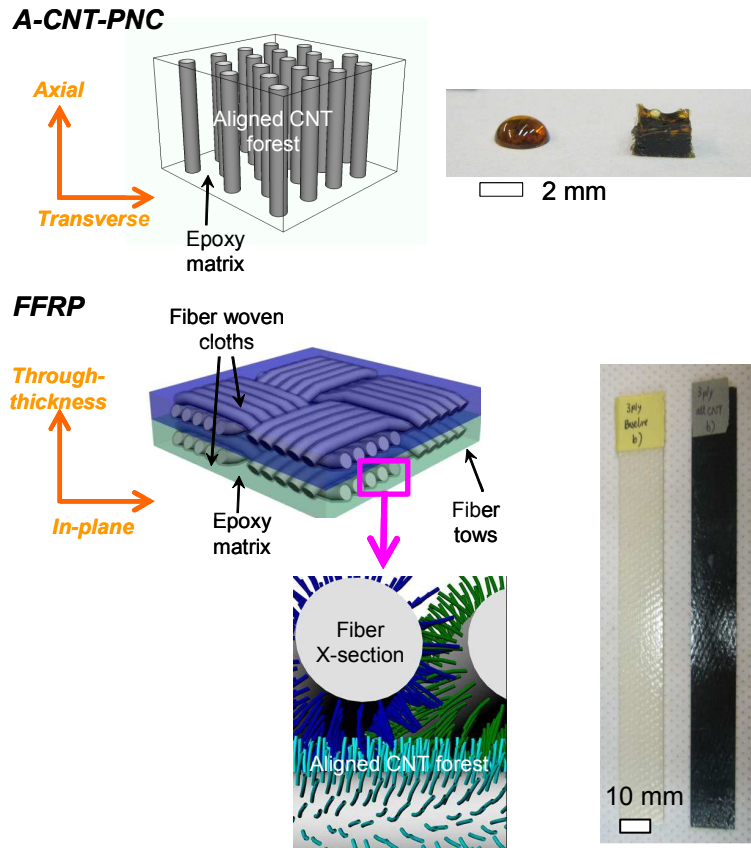


Figure 2. Schematics and photos of aligned CNT polymer nanocomposite (top) [27-28] and CNT hybridized fuzzy fiber-reinforced plastic (FFRPs, bottom) [14]. Illustrations not to scale.

II. Fabrication of FFRPs and A-CNT-PNCs

The nano-engineered composite studied in this work has been developed as illustrated in Fig. 2 [14], consisting of three-phases; advanced fibers (high volume fraction of ~60%), polymer matrix, and aligned CNTs. The laminate structure employ dense, uniformly distributed, and radially aligned CNTs grown *in situ* on the individual fiber surface of woven alumina cloth [40]. This nano-/micro-structure has two major advantages. First, aligned CNTs grown on adjacent fibers interact with one another inside and in-between the stacked layers, forming conductive pathways (and mechanical bridging) throughout the composites. Second, the fabrication method is potentially scalable, using catalyst application by dip-coating, mass MWNT production using chemical vapor deposition (CVD) with iron catalyst, and traditional lay-up composite fabrication (the details in [14, 40]). Note that aligned CNTs are only one possible morphology of in situ grown CNTs on the alumina fibers, other morphologies are possible if care is not taken [40] in the CVD processing. In addition, aligned CNTs remain attached to the fibers during capillary-infiltration with polymer (Resin 105, West Systems), and remain well dispersed. CNTs are thus introduced in an ordered way to composites, unlike the conventional way of mixing CNTs into epoxy materials that causes agglomeration, damage, and fracture. Alumina fibers are chosen for this model composite because alumina substrate and iron catalyst works well for CNT growth, and also because no damage to these alumina fibers was observed during single-fiber tensile testing [23, 41]. Significant mechanical property enhancement has been observed for the FFRP composites, including 1.5 kJ/m² enhancement of steady-state Mode I fracture toughness, in prior work [14, 42].

A-CNT-PNCs are fabricated, taking advantage of a capability of repeatable growth of continuous aligned CNTs, and independent variation of their length and volume fraction (a unique capability), minimizing uncertainty in sample characterization. Vertically aligned CNTs are grown on silicon substrates through CVD, and are well characterized for their quality, geometry, and alignment [43-45]. CNT forests are mechanically densified and then wet with epoxy (HexFlow RTM6, HEXCEL) again using capillary forces [28, 46]. With the size of these samples, even some bulk characterization methods can be applied, unlike unsupported aligned CNT forests that require elaborate sample preparation efforts. Fabricated samples are shown in Fig. 2. In addition to CNT composites, baseline composites that consist of pure epoxy (for A-CNT-PNCs) and that consist of alumina fibers and epoxy (for FFRPs) without CNTs were fabricated and tested to evaluate enhancement by CNT implementation.

III. Electrical and Thermal Testing of FFRPs

FFRP samples are tested for their electrical and thermal conduction in both through-thickness and in-plane directions. More than one method is employed to increase validity of measured data of these unique composites. Also, alumina-fiber reinforced plastics without CNTs, fabricated in the same way as FFRPs, are characterized as baseline composites to evaluate enhancement due to CNT implantation.

A. Electrical Conductivity

Electrical properties of FFRPs were characterized through three methods: DC electrical resistivity measurement (ASTM D257-99), AC impedance measurement (ASTM D150-98), and DC four-probe measurement (ASTM F390-98). For the first two methods, silver (Ag) paint (Structures Probe Inc.) was applied to the relevant surfaces of the composite as electrodes. DC volume resistances are characterized from repeated I-V

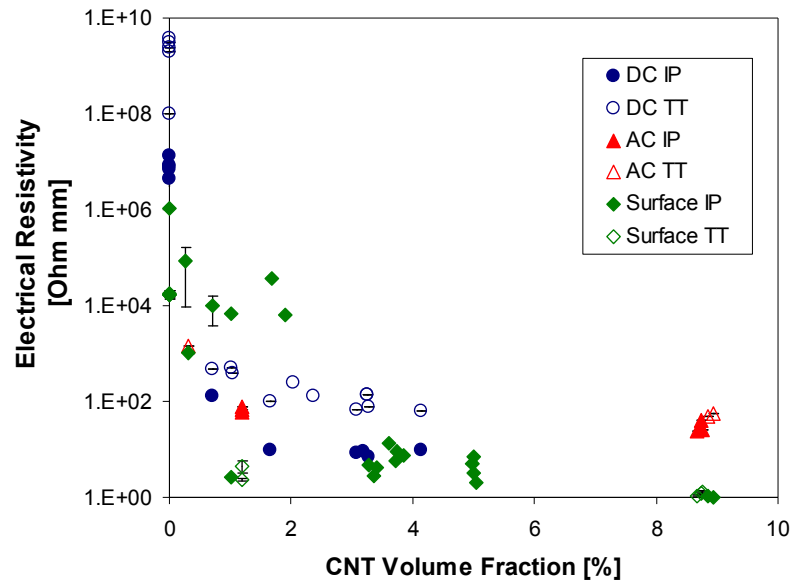


Figure 3. Electrical resistivity of FFRPs measured with DC volume (DC), AC impedance (AC), 4probe (Surface) methods in both in-plane (IP) and through-thickness (TT) directions.

curves on samples [47]. AC impedances are measured through an impedance analyzer (10Hz-40MHz, HP impedance /gain-phase analyzer 4194A) [48, 49], and resistivity values for comparison with the DC volume value are obtained through the real parts of measured impedances. As-fabricated samples (without Ag paint electrodes) are used for the four-probe measurement (Keithley, S-302-4), and resistivity values for comparison with the DC volume value are extracted using the appropriate correction factor from the raw data [50, 51]. On each sample, measurements are repeated at least 3 times at different locations.

Measured electrical resistivity values of FFRPs are summarized in Fig. 3. DC electrical resistivity rapidly decreases with a small CNT volume fraction ($\sim 0.5\%$ volume fraction V_f), indicating percolation occurs below this CNT V_f . Once CNT networks are formed through the structure, the conductivity improvement becomes nearly linear. With the small CNT addition ($\sim 0.5\text{-}3\text{ wt}\%$), conductivity increase by a factor of $10^6\text{-}10^8$. Electrical conductivities of FFRPs with $\sim 3\%$ CNT V_f are measured to be $\sim 120\text{ S/m}$ (in-plane, $\times 10^6$ of baseline) and to be $\sim 13.6\text{ S/m}$ (through-thickness, $\times 10^7$ of baseline), showing that FFRPs can be employed as EMI shielding ($>10\text{ S/m}$). In comparison, values estimated from AC impedances and surface resistances show the same trends and ranges with the DC measured values. However, some data measured in the in-plane directions using 4 probes show higher resistances with low CNT volume fractions ($\sim 2\%$ CNT V_f), and this can be attributed to epoxy-rich regions on the sample surfaces where the probes made contacts.

B. Thermal Properties

Thermal diffusivity and heat capacity of FFRPs are measured via the laser-flash method (based on ASTM E1461-07) in the through-thickness direction [49]. First, sample geometry was prepared so that the samples fit on the measurement stage (NETZSCH, microflash LFA457) to have the same geometry as the reference sample (SP-1 Vespel, 12.66 mm diameter, and 1.023 mm thickness). FFRP laminates (1 or 2 ply) were core-drilled into a circular disc ~ 1.25 mm-diameter, and then the discs were polished down (Struers, $\sim 5\text{ }\mu\text{m}$ roughness) to ~ 1 mm thickness. In laser flash method, the front side of the sample was heated using a laser pulse (InSb, maximum 15 J, 0.33 ms), and the temperature profile on the opposite side of the specimen was measured with an infrared detector over time. Thermal diffusivity is calculated from the time required to cool down (to half the maximum temperature) and the sample thickness. The sample temperature profile is also used to obtain the initial temperature increase, from which heat capacity is obtained. Thermal conductivity is calculated as the product of the measured thermal diffusivity and heat capacity and the known specimen density. The data extraction analysis used is for isotropic media and does not take into account differences due to in-plane vs. through-thickness property variation which may be present in the laminated woven FFRP composite.

Measured heat capacity has a relatively constant value of $\sim 1.1\text{ J/gK}$ regardless of CNT volume fraction, while thermal diffusivity shows a slight increase from 0.3 (baseline) to $0.7\text{ mm}^2/\text{s}$ ($\sim 4.4\%$ CNT V_f). Accordingly, thermal conductivity, with the error range estimated as $< \sim 3\%$, is estimated as 0.64 W/mK (through-thickness, $\times 1.9$ of baseline) with $\sim 3\%$ CNT V_f , as shown in Fig. 4, which is much smaller than metals ($\sim 100\text{s}$ of W/mK). Enhancement effect by CNT inclusion is much lower than that of electrical conduction or expectation [52]. This behavior can be attributed to different mechanisms of thermal vs. electrical transport, because in thermal transport thermal barrier resistances (TBRs) between the CNTs [53] play significant roles. Another explanation specific to the samples is that thermal transport is likely interrupted by the large volume fraction of insulating alumina fibers

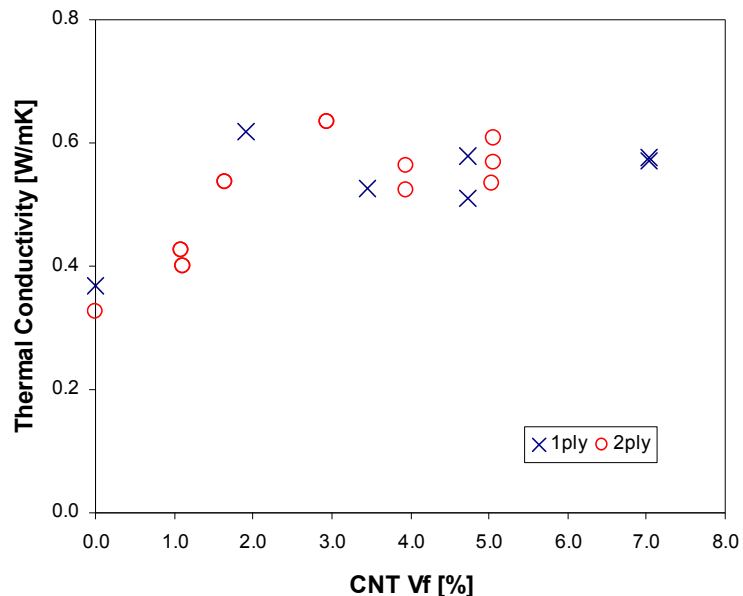


Figure 4. Thermal conductivity of FFRPs (1-ply and 2-ply) in the through-thickness direction measured with laser flash method.

($\sim 40\% V_f$) [54]. To achieve the case of continuous CNT conducting channels resulting in high (~ 100 s of W/mK) thermal conduction [52], structural or chemical modification of the FFRPs can be pursued in the future to obtain an improved thermal CNT network. In-plane thermal conductivity measurements using a comparator method based on ASTM E1225 are underway.

IV. Characterization and Testing of A-CNT-PNC Representative Volume Elements

Characterization of the aligned CNT polymer nanocomposites (A-CNT-PNCs) in both directions (axial and transverse, as shown in Fig. 2) is on-going, to seek trends caused by the parameters in electrical and thermal transport in comparison with theoretical expectations. Although property enhancement is observed with CNT addition, as seen when compared with Fig. 1, measured values do not reach the original expectations. Simple A-CNT-PNC samples (~ 1 -mm size) are characterized in order to fill in these knowledge gaps between macro-scale FFRPs and nano-scale CNT forests. Some characterization methods are developed in order to accommodate these small, anisotropic samples based on ASTM standards and other established methods.

A. Electrical Conductivity

Electrical characterization of A-PNCs compares bulk and local measurement on the same sample sets. Bulk volume measurement is based on (ASTM D257-99), with two major original modifications that are still compatible with the ASTM. The first modification is the electrodes. The Ag paint used to characterize the FFRPs has $\sim \mu\text{m}$ -sized metal particles, and its thickness is difficult to control. These characteristics are compatible with macro-scale samples like FFRPs, but with small samples like A-CNT-PNCs and when trying to achieve direct contact to CNT ends, Ag paint is not ideal. In order to minimize contact resistance and enhance contact to CNTs rather than the polymer, sample surfaces were polished (Struers down to $0.3 \mu\text{m}$, and then Vinromet, Buehler, with 60 nm). When observed under atomic force microscopy (Nanosurf EasyScan 2, nanoScience Instruments), the surface roughness average is $\sim 5 \text{ nm}$ as shown in Fig. 5 (vs. CNT diameter of $\sim 8 \text{ nm}$ [55]). Then, a thin platinum (Pt) layer was deposited on the polished surface by sputtering (Kurt J. Lesker Company). Second, contact resistances are eliminated in analysis from consistent data sets on the same sample but with different thicknesses. In volume resistance measurement, raw data include the effect of resistances from materials in series with the sample (normally much smaller than the sample resistance, and can be ignored) and also the contact resistances between probes/wires and the sample or between electrodes and the sample. Assuming diffusive electron transport in multi-walled nanotubes with $\sim 1 \text{ mm}$ length, the resistances of A-CNT-

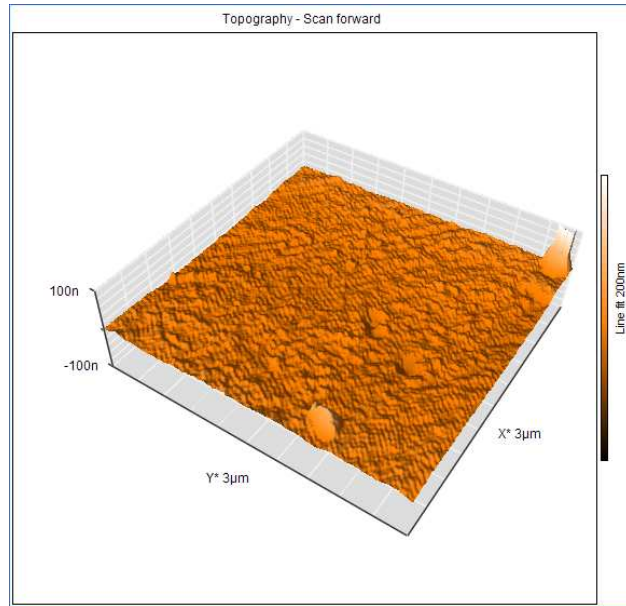


Figure 5. AFM image of the polished top surface of a transverse A-CNT-PNC ($\sim 8.7\% \text{ CNT } V_f$). Area roughness calculated as $\sim 3 \text{ nm}$.

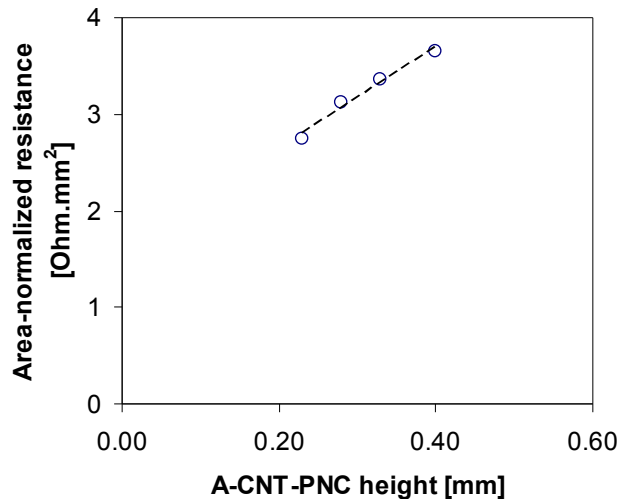


Figure 6. Area-normalized resistance variation measured with height decrease on a A-CNT-PNC (axial direction, $\sim 6.1\% \text{ CNT } V_f$).

PNCs are expected to linearly decrease with the sample height (the CNT length). After the first measurement on a sample, the same sample was roughly polished to a shorter height, and then precision surface polishing and Pt electrode deposition were repeated. On one sample, resistances with at least three different heights are measured. An example of such repeated measurement on varying sample height is shown in Fig. 6.

Electrical conductivities of A-CNT-PNCs with various CNT volume fractions are compared with previous measurements done by other groups on CNT-polymer nanocomposites [20, 21, 24, 25, 32, 33] in Fig. 7. Two key observations are made with these results. First, the electrical conductivity increase linearly, unlike percolation behaviors (rapid increase in conduction at a certain particle loading) observed with FFRPs above or with polymer nanocomposites (with randomly oriented CNTs) in the literature. On the contrary, CNTs are aligned inside these A-CNT-PNCs, and thus aligned CNTs act as direct conducting channels, an effect operating at all volume fractions. Second, electron conduction in both axial and transverse directions is higher for CNT-polymer nanocomposites than all reported in the extant literature. Higher electron transport in the direction perpendicular to the CNTs even with the small loading can be attributed to preservation of CNT quality or uniformity of CNT distribution due to the way A-CNT-PNCs are fabricated (capillary-driven wetting). Meanwhile, further analysis of the data is planned to evaluate the inter-CNT hopping resistances, etc. When the resistance of an individual CNT is extracted simply by multiplying the A-CNT-PNC resistance with the number of CNTs inside, the resistance is on the order of 10^9 Ohm, and this value is higher than resistances when experimentally measured individually (10^2 - 10^8 Ohm per ~ 1 μm -long multi-walled CNT) [56-60]. In order to understand the effect of polymer on the transport behavior and the scaling effect, a new local measurement technique is being employed.

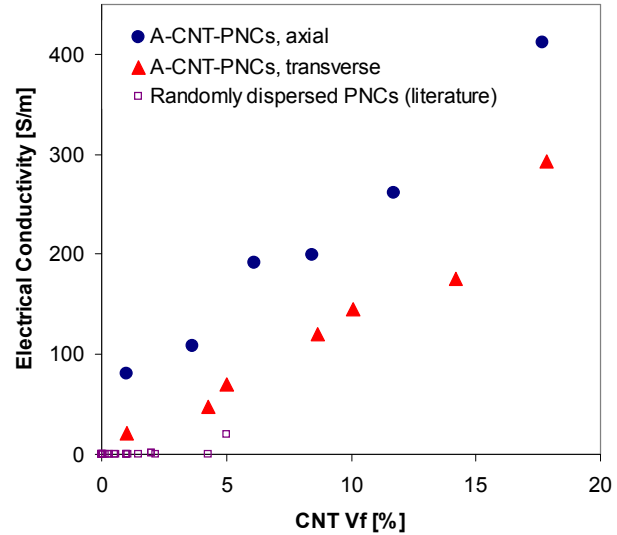


Figure 7. Electrical conductivity of A-CNT-PNCs in the axial and transverse directions, after elimination of contact resistances, compared with the measured values of randomly oriented CNT-nanocomposites from the literature [20, 21, 24, 25, 32, 33].

B. Thermal Conductivity

A variety of measurement methods have been used to measure thermal conductivity of CNTs and CNT-polymer nanocomposites. The principle of all the methods is the same: heat is supplied to a sample, and thermal conduction is measured based on temperature (gradient over time or space). Criteria of measurement method selection normally consists of measurement range (thermal conductivity, and temperature), material compatibility (anisotropy, electrical property if resistively heated, etc.), and more. For small-sized samples, measurement resolutions and minimal handling and disturbance to samples are key evaluation factors. Samples with small thermal mass are easy to heat, but their temperature gradients are more difficult to measure over small dimensions. In addition, unless heat losses are properly evaluated, temperature of the samples are easily affected by the environments (convection or conduction through materials in contact like thermocouples), which can result in inaccurate conductivity measurement. Employment of suitable measurement methods (preferably with heating that does not involve with direct electric current supply, and with non-contact temperature measurement) and accompanying analyses are crucial.

For on-going A-CNT-PNCs bulk conductivity measurement, a comparator method based on ASTM E1225-04 is employed with a high resolution infrared camera, to minimize physical contacts to the samples and to visualize thermal resistances at interfaces. For rather local measurement on the order of $\sim \mu\text{m}$ -sized spots, the pico-second thermoreflectance method is being used on Pt-deposited surfaces.

V. Conclusions and Recommendations

Carbon nanotubes (CNTs) are a potential new component to be incorporated into existing aerospace structural composites for multifunctional property enhancement. Improvements of traditional advanced composites, consisting of advanced fibers and matrices, are desired in mechanical and non-mechanical aspects of these composites; electrical conductivity and thermal conductivity as focused on in this work. Although CNT properties are promising when measured individually, those properties are mitigated by a large factor when integrated in structural systems (often polymer matrices as considered here). Mechanisms and effectiveness of nano-scale CNT implementation into macro-scale composites are therefore not well understood. Theoretical studies, both analytical and numerical, have been recently developed, suggesting boundary effects may be a key to explaining the above limitations, including electron tunneling/hopping or phonon scattering at CNT-CNT and CNT-polymer interfaces. In this work, a multi-scale approach is taken to understand the above scaling effects. A CNT hybridized fiber polymer composites (FFRP) is developed that achieves uniform CNT distributions for thermal and electrical conductive network, and that allows scalable fabrication, to be further improved with infusion processes [61]. With small CNT inclusion ($\sim 0.5\text{-}8\% V_f$), characterization shows significant enhancement in electrical conduction ($\times 10^6\text{-}10^8$) but limited enhancement in thermal conduction ($\times 1.9$). In order to understand transport behaviors, a smaller and simpler CNT composite, an aligned CNT polymer nanocomposite (A-CNT-PNC) has been developed and investigated. The work is currently on-going with suitable methods for such small samples, with electrical conductivity beyond all other reported values observed of the A-PNCs due to the control of morphology and testing controls. The A-CNT-PNC architecture can be extended to other matrices for high temperature applications to improve flame resistivity, thermal stability [62], and fire-smoke-toxicity [63]. Applications of this three-dimensional hierarchical CNT-composite with improved electrothermal properties are numerous, from heaters for airplane surface deicing and anti-icing to structural health monitoring [26].

Acknowledgments

This work was supported by Airbus S.A.S., Boeing, Embraer, Lockheed Martin, Saab AB, Spirit AeroSystems, Textron Inc., Composite Systems Technology, and TohoTenax through MIT's Nano-Engineered Composite aerospace Structures (NECST) Consortium, and by the Linda and Richard (1958) Hardy Fellowship. The authors gratefully acknowledge A. John Hart (Univ. of Michigan), Enrique J. Garcia, John Kane, Carl V. Thompson, Amy Marconnet (Stanford Univ.), Kenneth Goodson (Stanford Univ.), Robert Mitchell, Gang Chen, Hohyun Lee, and George D. Whitfield for valuable discussion and technical support.

References

- ¹Panel on Small Spacecraft Technology, *Technology for Small Spacecraft*. 1994, National Academies Press: Washington, D.C. pp. 42-49.
- ²Ashby, M., *Materials Selection in Mechanical Design*, 3rd edition ed, Butterworth-Heinemann, 2005.
- ³Louis, M., S.P. Joshi, and W. Brockmann, "An Experimental Investigation of through-Thickness Electrical Resistivity of Cfrp Laminates," *Composites Science and Technology*, Vol.61, No.6, 2001, pp. 911-919.
- ⁴Davis, J.R., *Asm Specialty Handbook: Copper and Copper Alloys*, ASM International, 2001.
- ⁵*Mil-Std-1757a Military Standards: Lightning Qualification Test Techniques for Aerospace Vehicles and Hardware*. 1978, Department of Defense.
- ⁶*Dod-Std-1795 Military Standards: Lightning Protection of Aerospace Vehicles and Hardware*. 1986, U. S. Air Force.
- ⁷Gardiner, G., *Lightning Strike Protection for Composite Structures*, in *High Performance Composites*. 2006.
- ⁸Brown, R., *Handbook of Polymer Testing: Physical Methods*, Plastics Engineering, ed. R. Brown, Vol. 50, CRC, 1999.
- ⁹Diao, J., D. Srivastava, and M. Menon, "Molecular Dynamics Simulations of Carbon Nanotube/Silicon Interfacial Thermal Conductance," *The Journal of Chemical Physics*, Vol.128, No.16, 2008, pp. 164708-5.
- ¹⁰Gaier, J.R., et al., "The Electrical and Thermal Conductivity of Woven Pristine and Intercalated Graphite Fiber-Polymer Composites," *Carbon*, Vol.41, No.12, 2003, pp. 2187-2193.
- ¹¹Rolfes, R. and U. Hammerschmidt, "Transverse Thermal Conductivity of Cfrp Laminates: A Numerical and Experimental Validation of Approximation Formulae," *Composites Science and Technology*, Vol.54, No.1, 1995, pp. 45-54.
- ¹²Pilling, M.W., et al., "The Thermal Conductivity of Carbon Fibre-Reinforced Composites," *Journal of Materials Science*, Vol.14, No.6, 1979, pp. 1326-1338.
- ¹³Garcia, E.J., B.L. Wardle, and A.J. Hart, "Joining Prepreg Composite Interfaces with Aligned Carbon Nanotubes," *Composites Part A*, Vol.39, No., 2008, pp. 1065-1070.
- ¹⁴Garcia, E.J., et al., "Fabrication and Multifunctional Properties of a Hybrid Laminate with Aligned Carbon Nanotubes Grown in Situ," *Composites Science and Technology*, Vol.68, No.9, 2008, pp. 2034-2041.

- ¹⁵Guzman deVilloria, R., et al. "Model-Experiment Correlation for Mode I Interlaminar Toughening of Composite Interfaces Reinforced with Aligned Carbon Nanotubes," *17th International Conference on Composite Materials (ICCM)*, Edinburgh, Scotland, 2009.
- ¹⁶Smalley, R.E., et al., *Carbon Nanotubes: Synthesis, Structure, Properties and Applications*, Springer-Verlag, 2000.
- ¹⁷Saito, R., et al., "Electronic Structure of Graphene Tubules Based on C60," *Physical Review B*, Vol.46, No.3, 1992, pp. 1804-1811.
- ¹⁸Kane, C.L. and E.J. Mele, "Size, Shape, and Low Energy Electronic Structure of Carbon Nanotubes," *Physical Review Letters*, Vol.78, No.10, 1997, pp. 1932-1935.
- ¹⁹Gao, G., T. Cagin, and W.A.G. III, "Energetics, Structure, Mechanical and Vibrational Properties of Single-Walled Carbon Nanotubes," *Nanotechnology*, Vol.9, No.3, 1998, pp. 184-191.
- ²⁰McNally, T., et al., "Polyethylene Multiwalled Carbon Nanotube Composites," *Polymer*, Vol.46, No.19, 2005, pp. 8222-8232.
- ²¹Sandler, J.K.W., et al., "Ultra-Low Electrical Percolation Threshold in Carbon-Nanotube-Epoxy Composites," *Polymer*, Vol.44, No.19, 2003, pp. 5893-5899.
- ²²Park, K.Y., et al., "Application of MwnT-Added Glass Fabric/Epoxy Composites to Electromagnetic Wave Shielding Enclosures," *Composite Structures*, Vol.81, No.3, 2007, pp. 401-406.
- ²³Garcia, E.J., J.A. Hart, and B.L. Wardle, "Long Carbon Nanotubes Grown on the Surface of Fibers for Hybrid Composites," *AIAA Journal*, Vol.46, No.6, 2008, pp. 1405-1412.
- ²⁴Kim, P., et al., "Thermal Transport Measurements of Individual Multiwalled Nanotubes," *Physical Review Letters*, Vol.87, No.21, 2001, pp. 215502.
- ²⁵Kilbride, B.E., et al., "Experimental Observation of Scaling Laws for Alternating Current and Direct Current Conductivity in Polymer-Carbon Nanotube Composite Thin Films," *Journal of Applied Physics*, Vol.92, No.7, 2002, pp. 4024-4030.
- ²⁶Wicks, S., et al. "Tomographic Electrical Resistance-Based Damage Sensing in Nano-Engineered Composite Structures," *51st AIAA Structures, Structural Dynamics, and Materials (SDM) Conference*, Orlando, FL, 2010.
- ²⁷Garcia, E.J., et al., "Fabrication and Nanocompression Testing of Aligned Cnt/Polymer Nanocomposites," *Advanced Materials*, Vol.19, No., 2007, pp. 2151-2156.
- ²⁸Wardle, B.L., et al., "Fabrication and Characterization of Ultrahigh-Volume- Fraction Aligned Carbon Nanotube-Polymer Composites," *Advanced Materials*, Vol.20, No.14, 2008, pp. 2707-2714.
- ²⁹Jones, R.M., *Mechanics of Composite Materials*, Taylor and Francis, Inc., 1975.
- ³⁰Huang, H., et al., "Aligned Carbon Nanotube Composite Films for Thermal Management," *Advanced Materials*, Vol.17, No.13, 2005, pp. 1652-1656.
- ³¹Kovacs, J.Z., et al., "Two Percolation Thresholds in Carbon Nanotube Epoxy Composites," *Composites Science and Technology*, Vol.67, No.5, 2007, pp. 922-928.
- ³²Grossiord, N., et al., "On the Influence of the Processing Conditions on the Performance of Electrically Conductive Carbon Nanotube/Polymer Nanocomposites," *Polymer*, Vol.49, No.12, 2008, pp. 2866-2872.
- ³³Thostenson, E.T. and T.-W. Chou, "Processing-Structure-Multi-Functional Property Relationship in Carbon Nanotube/Epoxy Composites," *Carbon*, Vol.44, No.14, 2006, pp. 3022-3029.
- ³⁴Bauhofer, W. and J.Z. Kovacs, "A Review and Analysis of Electrical Percolation in Carbon Nanotube Polymer Composites," *Composites Science and Technology*, Vol.69, No.10, 2009, pp. 1486-1498.
- ³⁵Bekyarova, E., et al., "Multiscale Carbon Nanotube-Carbon Fiber Reinforcement for Advanced Epoxy Composites," *Langmuir*, Vol.23, No.7, 2007, pp. 3970-3974.
- ³⁶Mathur, R.B., S. Chatterjee, and B.P. Singh, "Growth of Carbon Nanotubes on Carbon Fibre Substrates to Produce Hybrid/Phenolic Composites with Improved Mechanical Properties," *Composites Science and Technology*, Vol.68, No.7-8, 2008, pp. 1608-1615.
- ³⁷Kepple, K.L., et al., "Improved Fracture Toughness of Carbon Fiber Composite Functionalized with Multi Walled Carbon Nanotubes," *Carbon*, Vol.46, No.15, 2008, pp. 2026-2033.
- ³⁸Qian, H., et al., "Hierarchical Composites Reinforced with Carbon Nanotube Grafted Fibers: The Potential Assessed at the Single Fiber Level," *Chemistry of Materials*, Vol.20, No.5, 2008, pp. 1862-1869.
- ³⁹Sager, R.J., et al., "Effect of Carbon Nanotubes on the Interfacial Shear Strength of T650 Carbon Fiber in an Epoxy Matrix," *Composites Science and Technology*, Vol.69, No.7-8, 2009, pp. 898-904.
- ⁴⁰Yamamoto, N., et al., "High-Yield Growth and Morphology Control of Aligned Carbon Nanotubes on Ceramic Fibers for Multifunctional Enhancement of Structural Composites," *Carbon*, Vol.47, No.3, 2008, pp. 551-560.
- ⁴¹Garcia, E.J., et al. "Fabrication and Testing of Long Carbon Nanotubes Grown on the Surface of Fibers for Hybrid Composites," *47th AIAA/ASME/ASCE/AHS/ASC Structures, Structural Dynamics, and Materials Conference*, Newport, RI, 2006.
- ⁴²Wicks, S.S., R.G.d. Villoria, and B.L. Wardle, "Interlaminar and Intralaminar Reinforcement of Composite Laminates with Aligned Carbon Nanotubes," *Composites Science and Technology*, Vol.70, No.1, 2010, pp. 20-28.
- ⁴³Hart, A.J., *Chemical, Mechanical, and Thermal Control of Substrate-Bound Carbon Nanotube Growth*, in *Mechanical Engineering Department*. 2006, Massachusetts Institute of Technology: Cambridge, MA.
- ⁴⁴Wang, G., et al., "Conducting MwnT/Poly(Vinyl Acetate) Composite Nanofibres by Electrospinning," *Nanotechnology*, Vol.17, No.23, 2006, pp. 5829-5835.
- ⁴⁵Wang, J. and J.-S. Wang, "Carbon Nanotube Thermal Transport: Ballistic to Diffusive," *Applied Physics Letters*, Vol.88, No.11, 2006, pp. 111909-3.

- ⁴⁶Cebeci, H., et al., "Multifunctional Properties of High Volume Fraction Aligned Carbon Nanotube Polymer Composites with Controlled Morphology," *Composites Science and Technology*, Vol.69, No.15-16, 2009, pp. 2649-2656.
- ⁴⁷Yamamoto, N., et al., *Fabrication and Multifunctional Characterization of Hybrid Woven Composites Reinforced by Aligned Carbon Nanotubes*, in *16th International Conference of Composite Materials (ICCM)*. 2007: Kyoto Japan.
- ⁴⁸Yamamoto, N. and B.L. Wardle. "Electrical and Thermal Properties of Hybrid Woven Composites Reinforced with Aligned Carbon Nanotubes," *49th AIAA/ASME/ASCE/AHS/ASC Structures, Structural Dynamics, and Materials Conference*, Schaumburg, IL, 2008.
- ⁴⁹Yamamoto, N., et al. "Mechanical, Thermal, and Electrical Properties of Woven Laminated Advanced Composites Containing Aligned Carbon Nanotubes," *17th International Conference on Composite Materials*, Edinburgh, UK, 2009.
- ⁵⁰Valdes, L.B., "Effect of Electrode Spacing on the Equivalent Base Resistance of Point-Contact Transistors," *Proceedings of the IRE*, Vol.40, No.11, 1952, pp. 1429-1434.
- ⁵¹Valdes, L.B., "Resistivity Measurements on Germanium for Transistors," *Proceedings of the IRE*, Vol.42, No.2, 1954, pp. 420-427.
- ⁵²Sihn, S., et al., "Enhancement of through-Thickness Thermal Conductivity in Adhesively Bonded Joints Using Aligned Carbon Nanotubes," *Composites Science and Technology*, Vol.68, No.3-4, 2008, pp. 658-665.
- ⁵³Wardle, B.L. "Nanocomposites and Nano-Engineered Composites Reinforced with Aligned Carbon Nanotubes," *17th International Conference on Composite Materials*, Edinburgh, Scotland, 2009.
- ⁵⁴Winey, K.I., T. Kashiwagi, and M. Mu, "Improving Electrical Conductivity and Thermal Properties of Polymers by the Addition of Carbon Nanotubes as Fillers," *MRS BULLETIN*, Vol.32, No., 2007, pp. 348-353.
- ⁵⁵Hart, A.J. and A.H. Slocum, "Rapid Growth and Flow-Mediated Nucleation of Millimeter-Scale Aligned Carbon Nanotube Structures from a Thin-Film Catalyst," *Journal of Physical Chemistry B*, Vol.110, No.16, 2006, pp. 8250-8257.
- ⁵⁶Dai, H., E.W. Wong, and C.M. Lieber, "Probing Electrical Transport in Nanomaterials: Conductivity of Individual Carbon Nanotubes," *Science*, Vol.272, No.5261, 1996, pp. 523-526.
- ⁵⁷Wei, B.Q., R. Vajtai, and P.M. Ajayan, "Reliability and Current Carrying Capacity of Carbon Nanotubes," *Applied Physics Letters*, Vol.79, No.8, 2001, pp. 1172-1174.
- ⁵⁸Martel, R., et al., "Single- and Multi-Wall Carbon Nanotube Field-Effect Transistors," *Applied Physics Letters*, Vol.73, No.17, 1998, pp. 2447-2449.
- ⁵⁹Frank, S., et al., "Carbon Nanotube Quantum Resistors," *Science*, Vol.280, No.5370, 1998, pp. 1744-1746.
- ⁶⁰Ebbesen, T.W., et al., "Electrical Conductivity of Individual Carbon Nanotubes," *Nature* Vol.382, No.6586, 1996, pp. 54-56.
- ⁶¹Ishiguro, K., et al. "Processing and Characterization of Infusion-Processed Hybrid Composites with in Situ Grown Aligned Carbon Nanotubes," *50th AIAA/ASME/ASCE/AHS/ASC Structures, Structural Dynamics, and Materials Conference*, Palm Springs, CA, 2009.
- ⁶²Kashiwagi, T., et al., "Nanoparticle Networks Reduce the Flammability of Polymer Nanocomposites," *Nature Materials*, Vol.4, No.12, 2005, pp. 928-933.
- ⁶³Koo, J., *Polymer Nanocomposites: Processing, Characterization, and Applications*, McGraw-Hill Professional, 2006.